

Preliminary Results on Refined Source Waveform Estimation

by Raul Estevez

1. Introduction

We present some preliminary tests of a technique to estimate the source waveform and the deconvolved (whitened) Noah's seismogram, based on the idea of minimizing the power of the colored Noah's seismogram ("Refined Source Waveform Estimation", see page 50). This approach to waveform estimation and multiple suppression should offer several advantages over our previous one ("Shot Waveform Estimation", February 26).

For one thing we obtain as a direct result both the waveform and the deconvolved Noah's seismogram (reflection coefficient sequence). The previous method formulated the problem in terms of the inverse shot waveform. Also, we hope that this technique will eventually handle situations such as shallow water multiples which could not be handled by our former method. Finally, it does not seem to require confusing steps such as defining special gates, weighting functions, shifts, etc., which will result in simpler and more general algorithms.

The basic idea is to consider the colored Noah's seismogram $U' = U'(B, R')$ as a function of the waveform B and the surface observed seismogram R' :

$$U' = BU = \frac{BR'}{B+R'} \quad , \quad (1)$$

where U is the whitened Noah's seismogram.

A poor estimate of B will produce a U' not totally free from surface multiples. Since these remaining multiples add power to the seismogram, Claerbout expected that the minimization of $\|U'\|^2$ with respect to B , would yield improved U' and B .

As shown, the non-linear least square approach to the problem, in the case of vertical propagation, leads to the minimization of the length of

$$U' + dU' = U' + (\partial U' / \partial B) dB = U' - U'^2 dB \approx 0 \quad (2)$$

In terms of an overdetermined system of equations, relation (2) looks as follows:

$$\begin{bmatrix} u_0^2 & & & & & & & \\ u_1^2 & u_0^2 & & & & & & \\ u_2^2 & u_1^2 & u_0^2 & & & & & \\ \cdot & u_2^2 & u_1^2 & u_0^2 & & & & \\ \cdot & \cdot & u_2^2 & u_1^2 & u_0^2 & & & \\ \cdot & \cdot & \cdot & \cdot & \cdot & & & \\ \cdot & \cdot & \cdot & \cdot & \cdot & & & \end{bmatrix} \begin{bmatrix} dB_0 \\ dB_1 \\ \cdot \\ \cdot \end{bmatrix} = \begin{bmatrix} u'_0 \\ u'_1 \\ u'_2 \\ \cdot \\ \cdot \\ \cdot \\ \cdot \end{bmatrix} \quad (3)$$

Then a recursion could be organized according to the following scheme:

$$dB_i \leftarrow U_i, U'_i, \text{ using relation (3)}$$

$$B_{i+1} \leftarrow B_i + dB_i \quad (4)$$

$$U_{i+1}, U'_{i+1} \leftarrow B_{i+1}, R_i, \text{ using Noah's relation (1)}$$

where i refers to the recursion number and not the vectors' components.

As one would expect, the choice of a "good" starting value is critical. One possibility is to try $B=0$ or $B=1, 0, 0, \dots$ and then define U and U' through (1). Also, we could try to start with $U = U' = R'$ and then use (1) to define B . As we shall see later, the main thing here is a start which is not too far from the final solution.

2. Some practical aspects of the computation

In all the synthetic examples I considered, I started with an initial waveform B equal to the rescaled, tapered beginning of the first primary (sea bottom). In order to get the proper scale factor (maximum value of the tapering function), the amplitudes of this primary and its respective multiples were compared. In the case of real data, an additional time varying factor should be introduced to account for geometrical spreading (\sqrt{t} for plane wave stacks or t for point source data). This initial choice is illustrated in the following diagram:

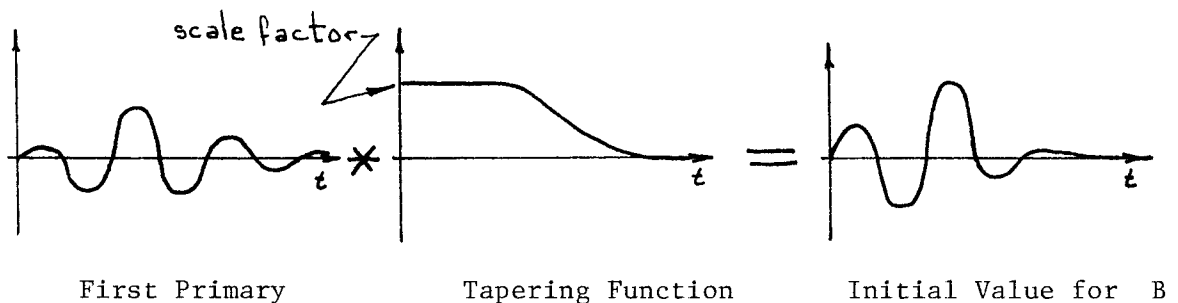


Figure 1.

The solution of the overdetermined system of equations (3) was computed using the subroutine LEVITY, described in Claerbout's paper, "Levity: Levinson Recursion Reprogrammed" (page 90). Since most of the synthetic data were too sparse, the minimization of the L_2 -norm was chosen over the median minimization. With the latter, the presence of too many zeros tends to produce zero medians.

Frequently, the denominator $B+R'$ in the Noah's expression (1) tends to be non-minimum phase, and consequently, the computation of U , U' and U^2 was done in the frequency domain. At this point I shall mention a very important constraint that was added to the recursion. We know that before the first reflector (sea bottom) the seismograms (R' , U' , U) should be zero. So upon transformation of U , U' and U^2 back into the time domain, we forced the equivalent number of zeros at the beginning of each one. Although we still do not understand fully the significance of this constraint, it was of extreme importance for convergence of the recursion. For example, in the computation of U^2 , a more stable convergence resulted, after forcing the zeros of U in the time domain (it would seem much simpler to compute U^2 at the same time we are computing U and U' in the frequency domain). This behavior probably is related to the familiar cyclic property of the discrete fourier transform when the vectors are chopped too early. Thus, by zeroing the beginnings we partially eliminate the noise introduced by this chopping. From the physical point of view, this could be related to requiring causality for some of the vectors.

To avoid division by zero in expression (1), the spectrum of $B+R'$ was increased a small amount whenever it approached zero. This was achieved using the following approximation:

$$a/b \cong a b^* / \text{MAX} 0(b^2, \epsilon \text{BIGGEST}(b^2)) , \quad (5)$$

where a and b are complex vectors, b^* is the complex conjugate of b and ϵ is a small positive number. The expression in the denominator reads: take the maximum number between the given value of b^2 and ϵ times the biggest value of vector b^2 . By making ϵ sufficiently small, we do not significantly distort the spectrum of b .

The degree of convergence was decided by evaluating $\|DB\|/\|B\|$, and in my case, recursions continued until this ratio was $< 10^{-3}$.

3. About the convergence of the recursions

Since it is a non-linear least square problem, we can't say much about convergence. Moreover, the few steps that I took trying to clarify this problem generated more questions and unexpected results than real answers.

The problem is complex not only because of its non-linearity, but also because of the additional constraint whose real significance we still do not fully understand (zeroing of the beginnings of the vectors, requiring B to have a relatively small length, etc.).

At least two general criteria can be given:

a) The kind of linearization used generates a Gauss-Newton type of recursion, which for convergence usually requires initial values reasonably close to the final solutions.

b) Convergence could be improved by replacing the expression $B_{i+1} = B_i + d B_i$ with $B_{i+1} = B_i + \lambda d B_i$, where parameter λ is chosen in such a way as to improve or correct the rate and direction of convergence (i.e., steepest descent method).

But the really interesting fact that emerged from the synthetic studies was that, although we are minimizing $\|U'\|^2$, the constraints force it to come to its proper final value no matter if we start from a smaller or larger value of $\|U'\|^2$, provided that it lies within a certain strip of convergence.

Let us assume that \bar{U}' and \bar{B} are the final solutions of the recursion, then two values of U' , (U'_1 and U'_2) appear to exist, such that $\|U'_1\| < \|\bar{U}'\| < \|U'_2\|$. Within this range, any initial value of U' will converge to \bar{U}' . The situation is illustrated in Figure 2.

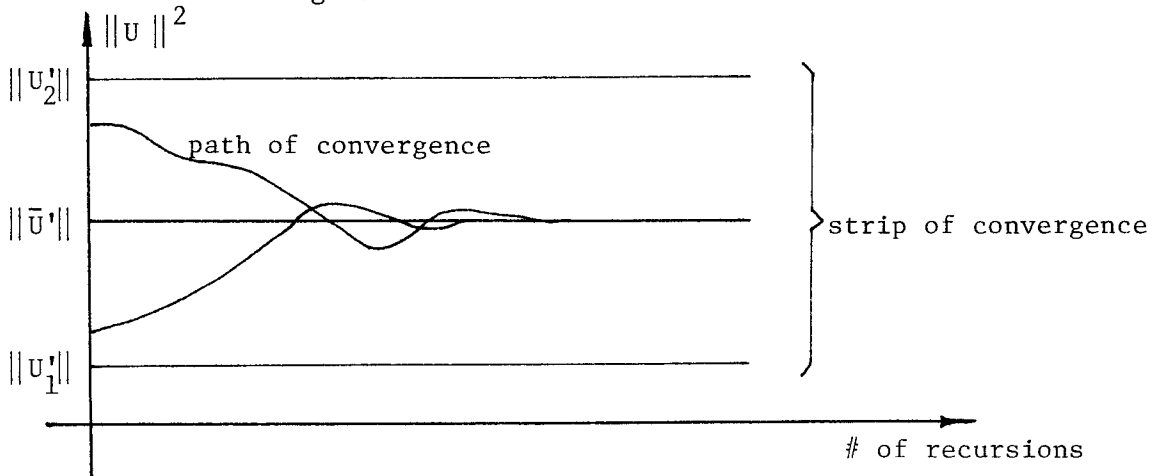


Figure 2.

Up to this point, no general way to define the strip of convergence has emerged.

This strange behavior probably is telling us that the constraints we are putting into the recursion play a more important role than the minimization by itself. Moreover, it explains why the most obvious and immediate solution $B=0$ and $U'=0$, do not emerge as a result of the recursion, since this case does not satisfy the constraints. In effect, if we assume $\|B\| \ll \|R'\|$, from (1) we have:

$$U = \frac{R'}{B+R'} = \frac{R'}{R'(1+\frac{B}{R'})} = 1 + f(B/R') \quad (6)$$

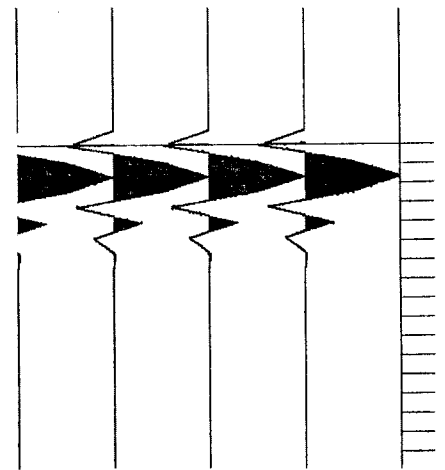
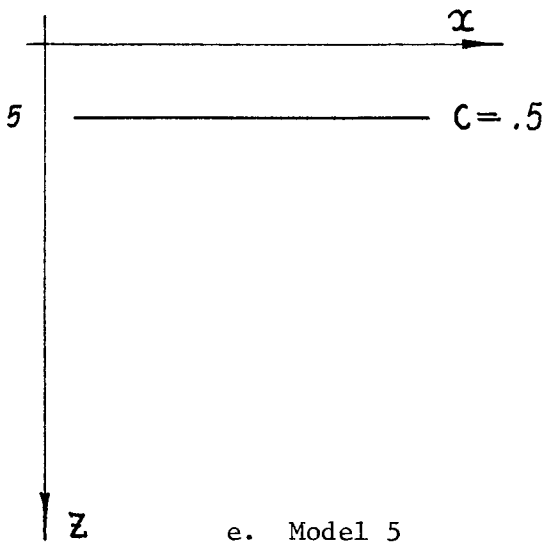
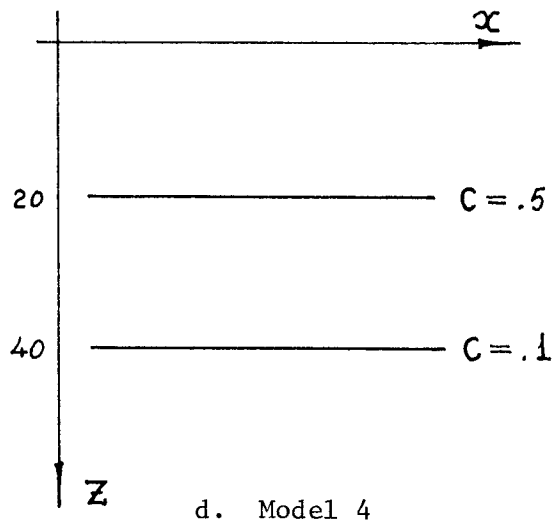
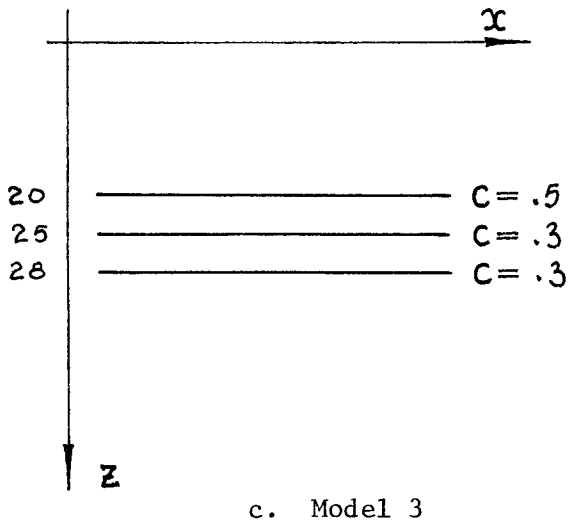
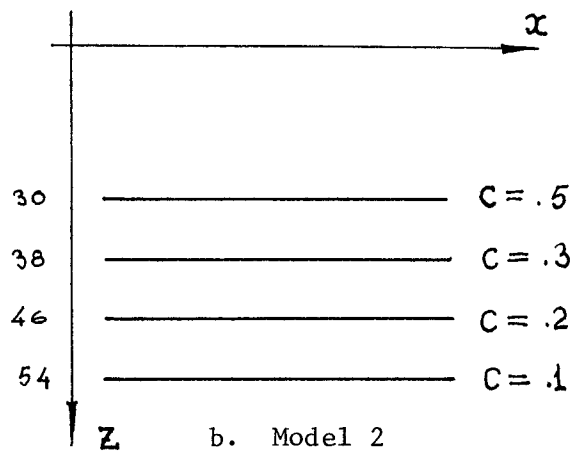
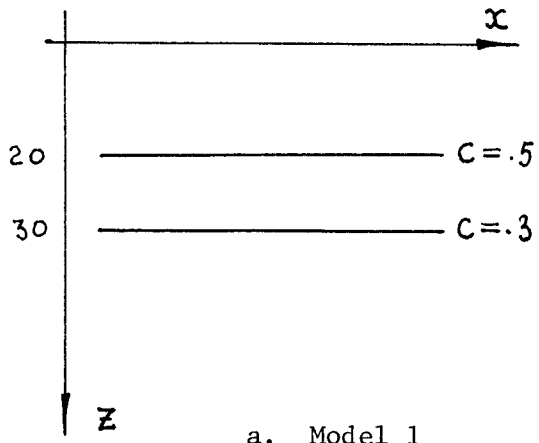
which tells us that $U \neq 0$ at $t=0$ (we are requiring causality for u ; that means $U=0$ for $t \leq 0$!)

The fact that $\|U'\|$ is not converging to a minimum in the common sense, makes even more difficult (but not impossible!) the proper choice of a convergence factor λ such as the one discussed above.

Therefore, it seems to me that considerably more work has to be put in this direction before it becomes a practical reality. On the other hand, the encouraging part of the story is that, as the following synthetics show, the technique works in principle.

4. Synthetic examples

In order to have a better feeling about the technique, its degree of resolution and its handling of relatively difficult situations, the following models were tested:



f. Synthetic shot waveform
 $B = (-.5, .5, 1., .5, -.4, .3, -.2)$

Figure 3.

In all the cases the same shot waveform (Fig. 3-f.) was used to produce the corresponding synthetic seismograms (Figs. 4 through 7) and the initial values for B , U and U' were chosen according to 2. Since we are considering only vertical propagation, the computation was done on a single trace, but for display purposes, this trace was repeated several times in Figures 4-7, after being convolved with 3 point binomial wavelet (1., 2., 1.) . All the synthetic seismograms were taken 150 points long.

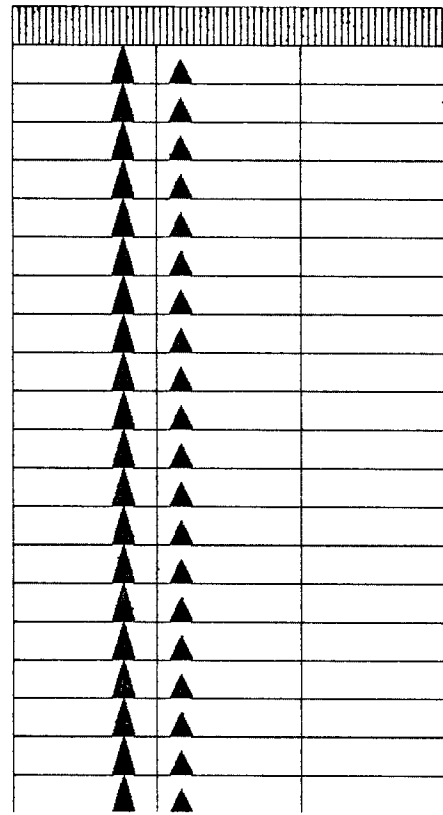
Model 1 is a "good" model, used mainly to test the technique in nearly optimal conditions. It took 9 iterations to achieve the desired degree of convergence ($\|DB\|/\|B\| < 10^{-3}$). The results are illustrated in Figure 4.

Model 2 was used to test the degree of resolution in relation to the strength of the reflectors. As we see in Figure 5, the final U (after 15 iterations) is reasonably good and only the last reflector was lost. The estimated waveform is not as good as in the previous case, however, this result could be greatly improved by extending the corresponding synthetic seismogram beyond 150 points, since the reflections have not died down at that time.

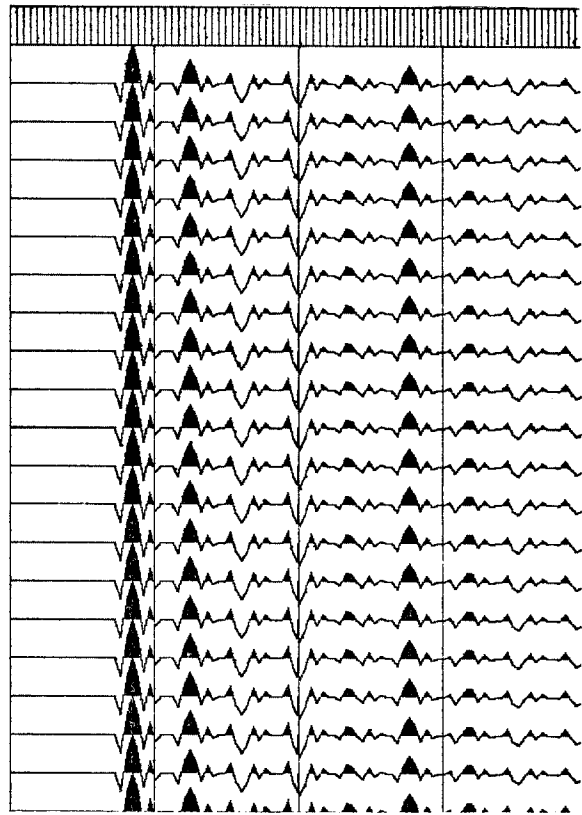
Model 3 was meant to test resolution in terms of separation among reflectors. The first 2 reflectors are 5 points apart and the last only 3 points apart (notice that the actual waveform is 7 points long). Figure 6 shows quite a good result both in terms of B and U .

Model 4 tries a difficult situation: a small primary coincides with the first multiple. As Figure 7 shows, our technique cannot handle this type of situation. The second reflector was washed away in the final U and the estimated waveform is rather poor.

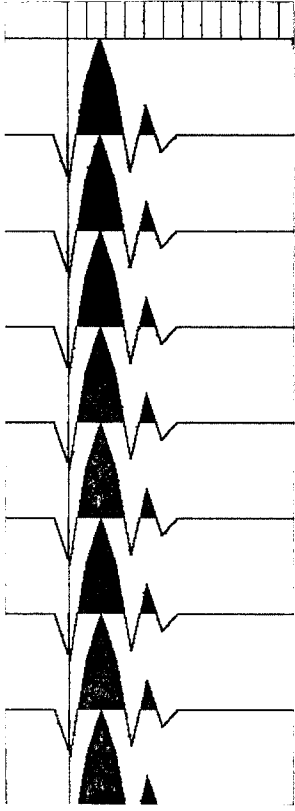
Model 5 tried another kind of difficulty, where we expected that this technique would be less sensitive than our previous one: shallow water. In this case the first multiple arrives before the first primary has died completely. Despite our expectations, the recursion flatly rejected the model: it diverged very quickly!



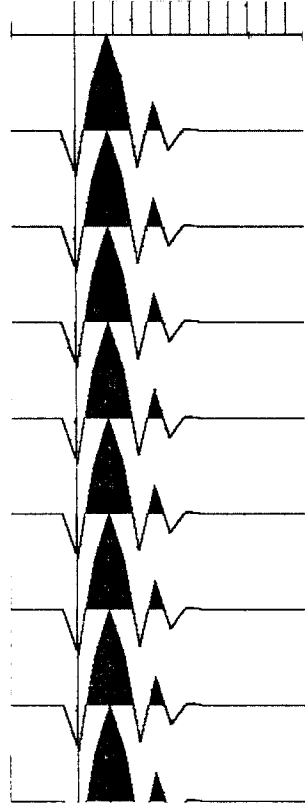
a. Model 1



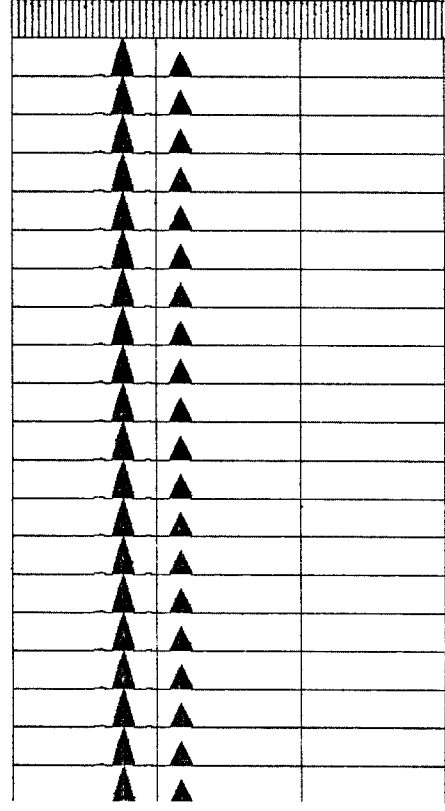
b. Synthetic seismogram



c. Synthetic shot waveform ($-.5, .5, 1., .5, .4, .3, -.2$)

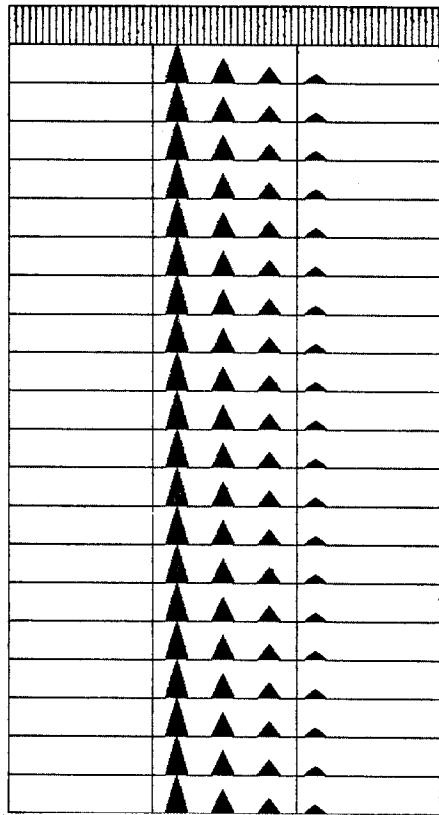


d. Estimated waveform

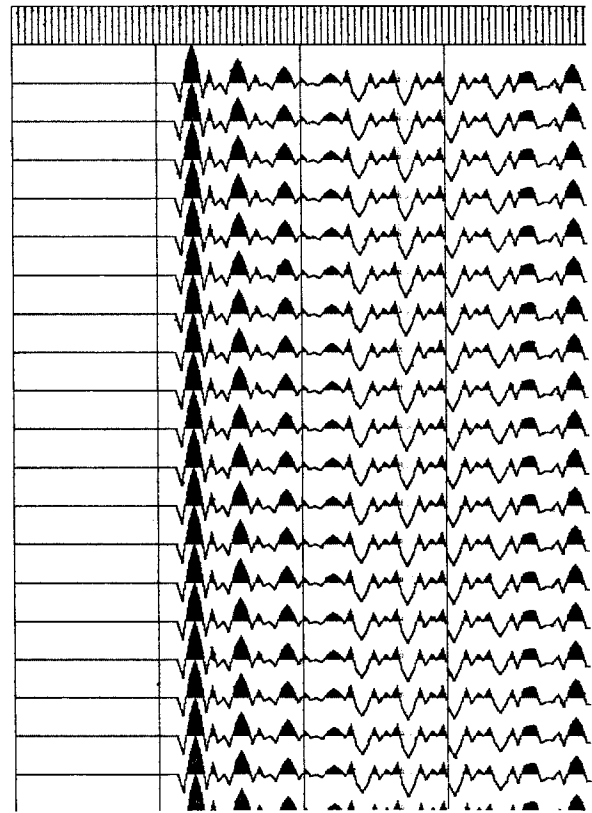


e. Estimated U (reflection coefficients).

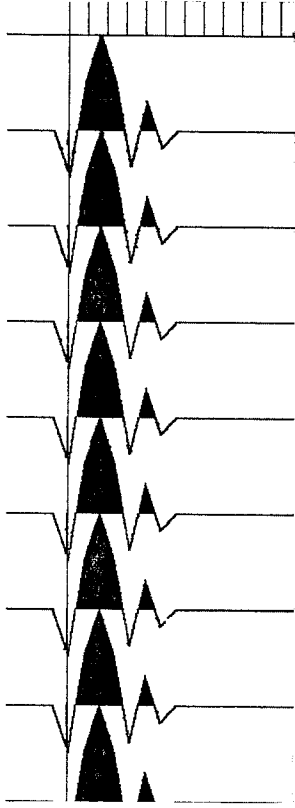
Figure 4.



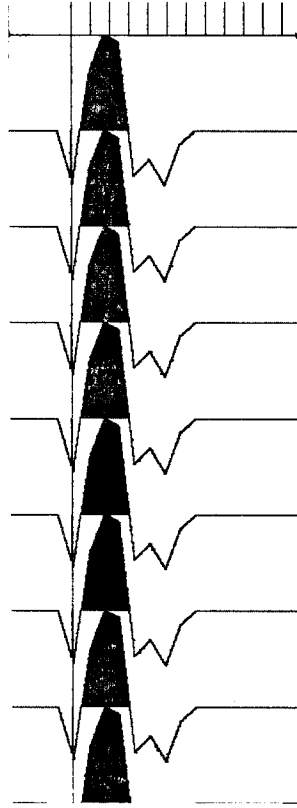
a. Model 2



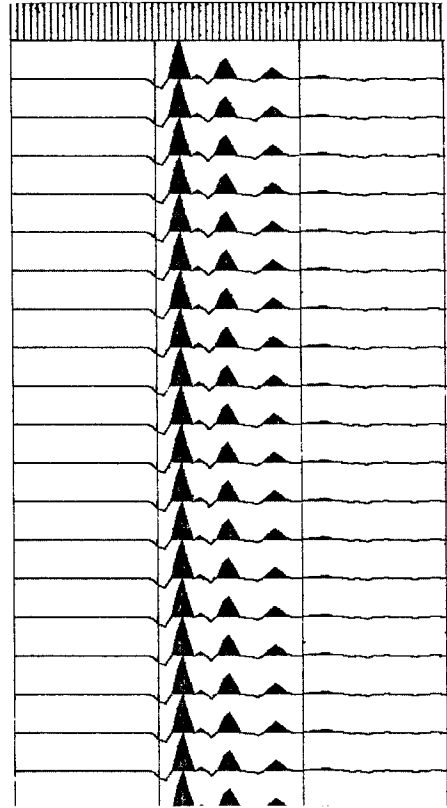
b. Synthetic seismogram



c. Synthetic shot waveform (-.5,.5,1.,.5,-.4,.3,-.2)

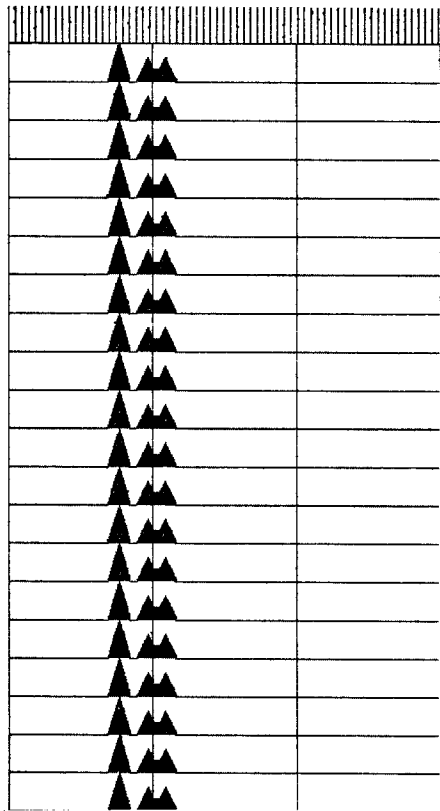


d. Estimated waveform

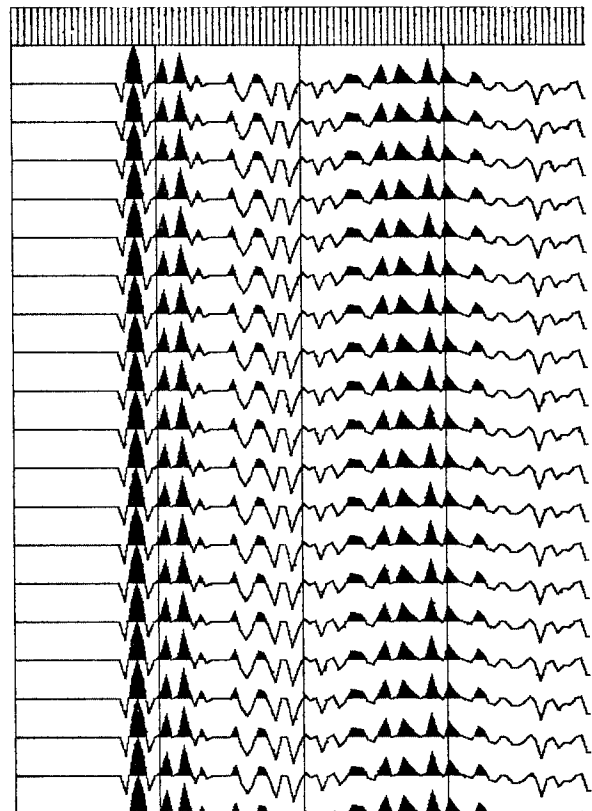


e. Estimated U (reflection coefficient)

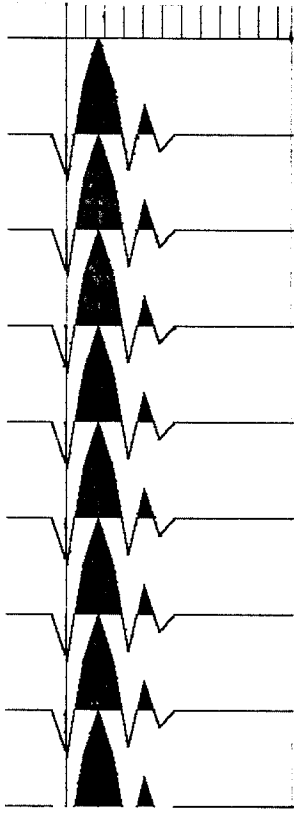
Figure 5.



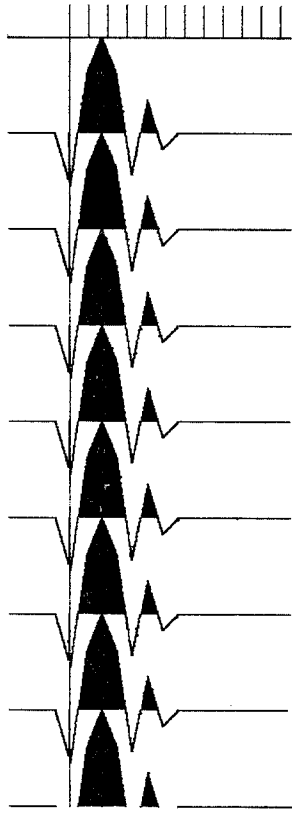
a. Model 3



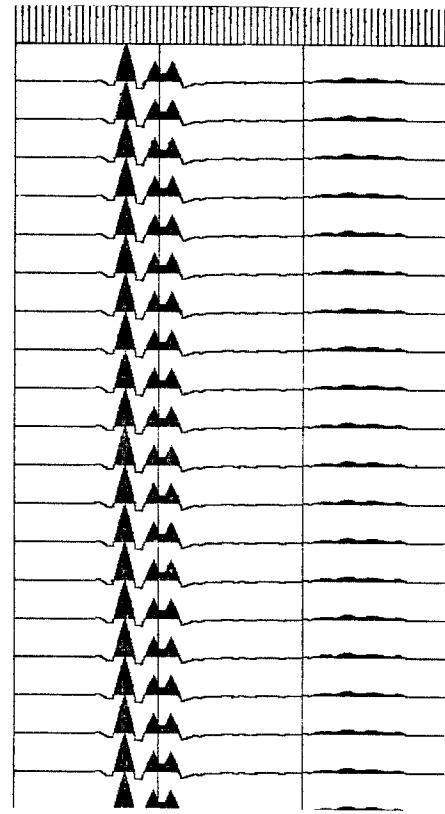
b. Synthetic seismogram



c. Synthetic shot waveform (-.5,.5,1.,.5,-.4,.3,-.2)

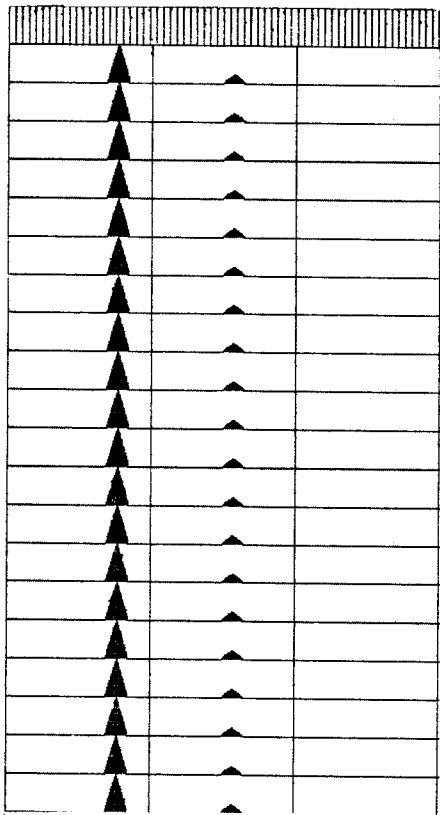


d. Estimated waveform

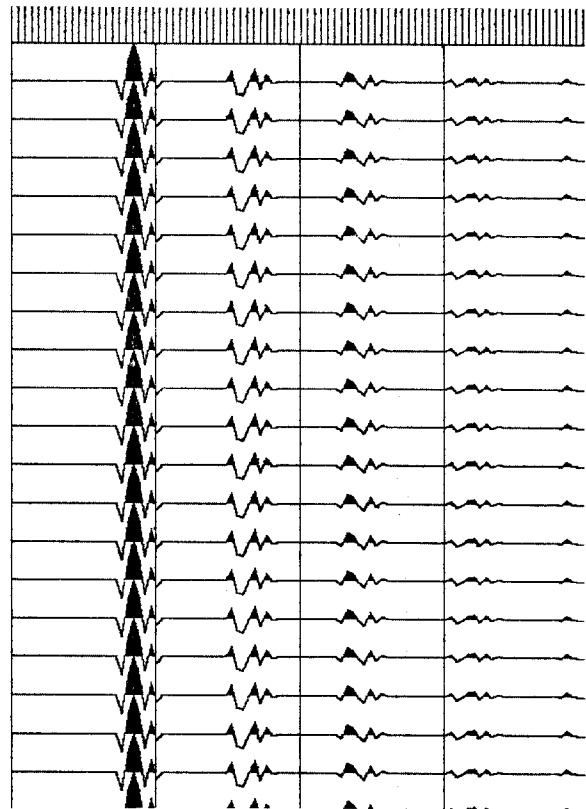


e. Estimated U (reflection coefficients)

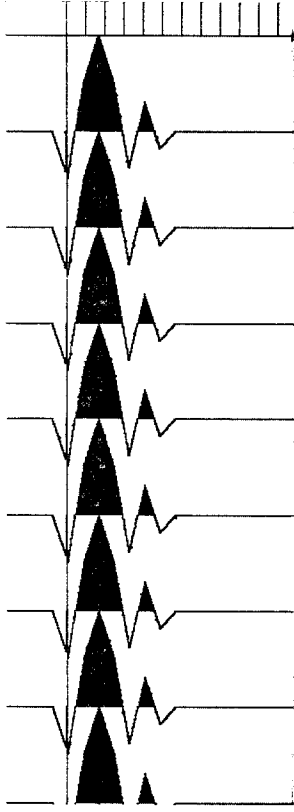
Figure 6.



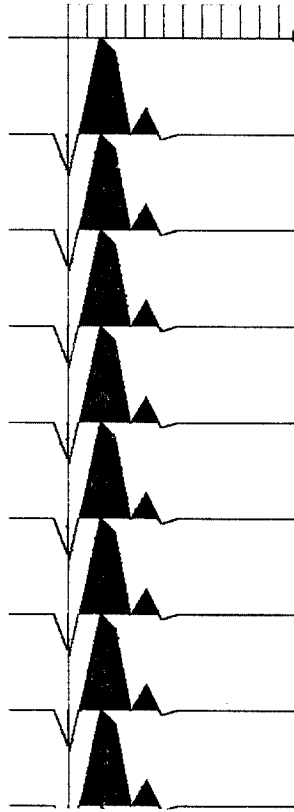
a. Model 4



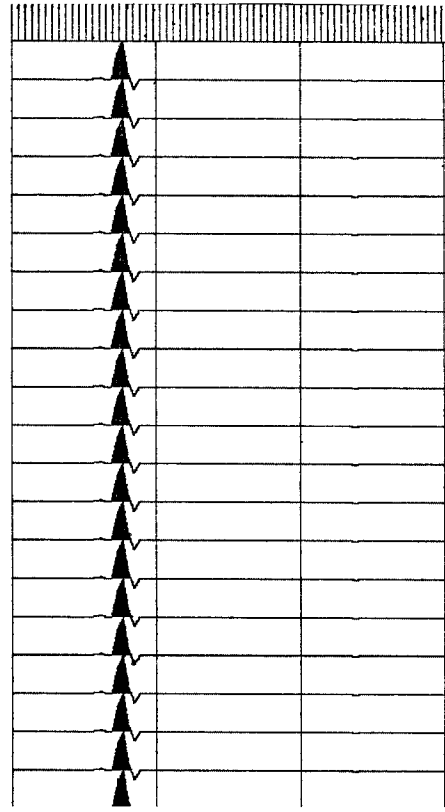
b. Synthetic seismogram



c. Synthetic shot waveform ($-0.5, 1.5, 3.5, 5.5, 7.5, 9.5, 11.5, 13.5, 15.5, 17.5, 19.5, 21.5$)



d. Estimated waveform



e. Estimated U (reflection coefficients)

Figure 7.